

# Pemafibrate suppresses oxidative stress and apoptosis under cardiomyocyte ischemia-reperfusion injury in type 1 diabetes mellitus

WEI LI<sup>1\*</sup>, JIANXIN XU<sup>1\*</sup>, XIN GUO<sup>1</sup>, XINHUA XIA<sup>2</sup> and YANLING SUN<sup>2</sup>

<sup>1</sup>Third Medical Department; <sup>2</sup>Nursing Department, Tianjin Teda Hospital, Tianjin 300457, P.R. China

Received April 9, 2020; Accepted October 14, 2020

DOI: 10.3892/etm.2021.9762

**Abstract.** Diabetes mellitus accelerates the hyperglycemia susceptibility-induced injury to cardiac cells. The activation of peroxisome proliferator-activated receptor  $\alpha$  (PPAR $\alpha$ ) decreases ischemia-reperfusion (IR) injury in animals without diabetes. Therefore, the present study hypothesized that pemafibrate may exert a protective effect on the myocardium *in vivo* and *in vitro*. A type 1 diabetes mellitus (T1DM) rat model and H9c2 cells exposed to high glucose under hypoxia and reoxygenation treatments were used in the present study. The rat model and the cells were subsequently treated with pemafibrate. In the T1DM rat model, pemafibrate enhanced the expression of PPAR $\alpha$  in the diabetic-myocardial ischemia-reperfusion injury (D-IRI) group compared with the D-IRI group. The infarct size in the D-IRI group was reduced following pemafibrate treatment relative to the untreated group. The disruption of the mitochondrial structure and myofibrils in the D-IRI group was partially recovered by pemafibrate. In addition, to evaluate the mechanism of action of pemafibrate in the treatment of diabetic myocardial IR injury, an *in vitro* model was established. PPAR $\alpha$  protein expression levels were reduced in the high glucose and hypoxia/reoxygenation (H/R) groups compared with that in the control or high glucose-treated groups. Pemafibrate treatment significantly enhanced the ATP and superoxide dismutase levels, and reduced the mitochondrial reactive oxygen species and malondialdehyde levels compared with the high glucose combined with H/R group. Furthermore, pemafibrate inhibited the expression of cytochrome *c* and cleaved-caspase-3, indicating its involvement in the regulation of mitochondrial apoptosis.

Pemafibrate also reduced the expression of nuclear factor- $\kappa$ B (NF- $\kappa$ B), the activation of which reversed the protective effects of pemafibrate on diabetic myocardial IR injury *in vitro*. Taken together, these results suggested that pemafibrate may activate PPAR $\alpha$  to protect the T1DM rat myocardium against IR injury through inhibition of NF- $\kappa$ B signaling.

## Introduction

Diabetes is a metabolic disease during which the pancreas loses the ability to secrete insulin, resulting in high blood sugar levels (1). Severe diabetes may lead to seizures, heart attack, stroke and coma (2). Most patients with type 1 or type 2 diabetes die from complications rather than from diabetes itself (3,4). Heart disease is the most common and deadliest complication among patients with diabetes (5). Among the types of heart disease in patients with diabetes, ischemic heart disease is the most common, followed by cardiac failure (6). Reperfusion injury is a common prognostic problem for percutaneous transluminal coronary intervention therapy (7). A previous study has demonstrated that myocardial ischemia-reperfusion (IR) injury (IRI) is induced in patients with diabetes more easily compared with that in healthy populations, which may be caused by the alteration of mitochondrial function and reactive oxygen species production (8).

Peroxisome proliferator-activated receptor  $\alpha$  (PPAR $\alpha$ ) activation has been reported to improve cardiac function and increase ATP production in myocardial IRI (9,10). PPAR $\alpha$  serves a protective role against cardiac IRI by regulating the expression of uncoupling protein-3 (11). A previous study has demonstrated that PPAR $\alpha$  activation depends on the decrease of glucose uptake and susceptibility to ischemic injury (12). NF- $\kappa$ B is a transcription factor involved in diverse cellular activities, including the cardiac IRI (13). A previous study has reported that NF- $\kappa$ B activation is induced by diabetic metabolic disorders with myocardial IRI, whereas inhibition of NF- $\kappa$ B reverses diabetic-IRI (D-IRI) (14). Emerging evidence demonstrated that PPAR $\alpha$  overexpression can inactivate NF- $\kappa$ B signaling (15).

Pemafibrate, a selective PPAR $\alpha$  modulator, is effective at regulating lipid and glucose metabolism in patients with type 2 diabetes mellitus (16). A growing body of literature has shown that pemafibrate protects against multiple diabetic complications, for instance diabetic retinopathy, endothelial

---

*Correspondence to:* Dr Xin Guo, Third Medical Department, Tianjin Teda Hospital, 65 Third Avenue, The Development Zone, Binhai New Area, Tianjin 300457, P.R. China  
E-mail: guoxintjd@163.com

\*Contributed equally

**Key words:** diabetes, myocardial ischemia-reperfusion injury, peroxisome proliferator-activated receptor  $\alpha$ , apoptosis, oxidative stress

dysfunction and cardiovascular disease (17,18). However, the exact effects of pemafibrate on D-IRI and the potential mechanisms remains to be elucidated. The present study aimed to investigate whether pemafibrate may protect against diabetic IRI *in vivo* and *in vitro*, and to examine the molecular mechanism of action of pemafibrate.

## Materials and methods

**Animals.** Male Sprague-Dawley rats (age, 7 weeks; weight, 220-300 g) were provided by the Tianjin Experimental Animal Center. Rats were housed in a 12 h light/dark cycle, and food and water was available *ad libitum* during the experimental period. A constant temperature and humidity of 25°C and 50%, respectively, was maintained. Rats were subjected to experiments following 2 weeks of acclimatization. All animal care and experimental procedures were in compliance with the guidelines of the International Guiding Principles for Biomedical Research Involving Animals of the Council for International Organizations of Medical Sciences. All experimental procedures were approved by the Ethical Committee of Tianjin Teda Hospital (approval no. EC-20190722-1039).

**Diabetic-myocardial IRI (D-IRI) model.** The D-IRI experimental model was established as previously described (19). Rats were administered a single dose of 65 mg/kg streptozotocin (STZ; Sigma-Aldrich; Merck KGaA) by tail vein injection. Following induction for 8 weeks, the fasting blood (50  $\mu$ l) were collected by caudal vein blood once a week and the concentration of fasting blood glucose was measured, with  $\geq 16.7$  mmol/l indicating successful establishment of the type 1 diabetes mellitus (T1DM) model. Subsequently, rats were anesthetized with an intraperitoneal injection of 50 mg/kg body weight pentobarbital. The rats were mechanically ventilated with air through a rodent ventilator followed by oral endotracheal intubation. The body temperature of the rats was maintained at  $37 \pm 0.5^\circ\text{C}$ . The thoracic cavity was opened between the fourth and fifth intercostal space of the left edge of the thoracotomy, and the heart of the rat was exposed after pericardial incision. A 7-0 silk thread was sutured around the left anterior descending coronary artery of the rat, 2 mm from the tip of the left auricle; 10 min later, when the thread was clamped and tightened, a snare that blocked the artery was formed. Following ligation, regional epicardial cyanosis appearance in the heart was observed as a sign of successful ischemia. At 30 min after the ischemia, coronary artery reperfusion was performed by releasing the clamp for 2 h. The behavior of the rats was observed every 20 min. The rats were randomly divided into two groups ( $n=6$  in each group): D-IRI and D-IRI + pemafibrate (intragastric administration; 1 mg/kg). Pemafibrate was administered immediately after IRI. If the rats went into shock, decreased activity, lethargy or dyspnea, the animals were euthanized prior to the experimental endpoint. The rats were euthanized by an overdose of sodium pentobarbital (200 mg/kg intraperitoneal injection), followed by exsanguination from the abdominal aorta; death was confirmed by respiratory and cardiac arrest.

**Detection of infarction size.** To observe the infarct area, 2,3,5-triphenyltetrazolium chloride (TTC) staining was

performed. The fresh hearts were cut into transverse slices (1-2 mm-thick) and stained with 1.5% TTC (Sigma-Aldrich; Merck KGaA) for 20 min at 37°C. Subsequently, the stained slices were then fixed with 4% formaldehyde for 24 h. The unstained pale area (infarct area) and TTC-stained red area (ischemic but viable myocardium) were evaluated through planimetry with the Image-Pro Plus 4.5 software (Media Cybernetics, Inc.).

**Immunohistochemistry.** Cardiac tissues were embedded in paraffin as previously described (20). Paraffin-embedded specimens (4- $\mu$ m-thick) were deparaffinized and rehydrated with a graded ethanol and xylene series at room temperature. Antigen retrieval was performed by heating the slides in 1 mmol/l EDTA (pH 8.0) for 30 min. After blocking with 10% normal goat serum (Wuhan Servicebio Technology Co., Ltd.) for 10 min at 37°C, slides were probed with primary antibodies targeting PPAR $\alpha$  (cat. no. ab215270; 1:200; Abcam) overnight at 4°C. Subsequently, a horseradish peroxidase (HRP)-conjugated goat anti-rabbit IgG (cat. no. ab6721; 1:1,000; Abcam) antibody was added, incubated for 1 h at room temperature and visualized using the eBioscience DAB Advanced Chromogenic kit (Thermo Fisher Scientific, Inc.). The immunohistochemical images were acquired using a light microscope (DMI3000; Leica, Microsystems, Inc.) at x200 magnification from five random fields.

**Transmission electron microscopy (TEM).** The mitochondrial morphology in the rat hearts was assessed using TEM. Following the fixation of heart sections (1x1x1 mm) with 2.5% glutaraldehyde, an ethanol gradient dehydration (30, 50, 70, 80, 85, 90 and 100% ethanol gradient for 15-20 min) was performed. The tissues were subsequently embedded in Epon 812 resin (Sinopharm Chemical Reagent Co., Ltd.). The heart slices (0.1- $\mu$ m) were stained with 2% uranylacetate and 1% lead citrate. Tissue sections were observed and photographed using a Hitachi TEM system (Hitachi, Ltd.) at x6000 magnification from three random fields.

**Cell culture and treatment.** The embryonic rat cardiomyocyte-derived cell line H9c2 was obtained from the Cell Resource Center, Institute of Basic Medicine, Chinese Academy of Medical Sciences and cultured in high-glucose DMEM (cat. no. 11965092; Thermo Fisher Scientific, Inc.) supplemented with 10% FBS (Gibco; Thermo Fisher Scientific, Inc.), 100 U/ml penicillin and 100  $\mu$ g/ml streptomycin at 37°C in a humidified incubator with 5% CO<sub>2</sub>. The cells (1x10<sup>6</sup> cells/well) were seeded into 6-well plates. Prior to the experiments, the cells were starved in 1% FBS-supplemented low glucose DMEM (cat. no. 11885076; Thermo Fisher Scientific, Inc.) for 24 h and divided into the following groups: i) Low glucose (control; final concentration, 5.5 mmol/l); ii) high glucose (HG; final concentration, 33 mmol/l); iii) HG + hypoxia/reoxygenation (HG + H/R); and iv) HG + H/R + 50 nmol/l pemafibrate (MedChemExpress). Briefly, when the cells reached 60% confluence, they were pre-treated with control or HG media for 48 h. Subsequently, the H/R model was induced by culturing the cells for 6 h in hypoxic conditions (95% N<sub>2</sub> and 5% CO<sub>2</sub>) with 1% FBS-DMEM, followed by 4 h of

reoxygenation in normal culture conditions. Pemafibrate was dissolved in DMSO (203.85 mmol/l) before being added to media.

**Cell transfection.** An NF- $\kappa$ B overexpression plasmid (NF- $\kappa$ B) and its empty negative control vector (NC) were purchased from Shanghai GenePharma Co., Ltd. H9c2 cells were seeded into 6-well plates at a density of  $1 \times 10^6$  cells/well 24 h prior to transfection and incubated overnight. Transfection (100 nmol/l) was performed using Lipofectamine<sup>®</sup> 2000 (Invitrogen; Thermo Fisher Scientific, Inc.) according to the manufacturer's instructions. Transfection efficiency was assessed using reverse transcription-quantitative (RT-q)PCR 24 h post-transfection.

**Detection of mitochondrial function.** Mitochondrial dysfunction was determined by detecting the mitochondrial ROS (mtROS) levels, ATP content, malondialdehyde (MDA) release and superoxide dismutase (SOD) activity. mtROS levels were detected by mitochondrial superoxide (MitoSOX; Invitrogen; Thermo Fisher Scientific, Inc.) staining. Briefly, H9c2 cells ( $1 \times 10^6$  cells) were cultured with 5 mmol/l MitoSOX in serum-free DMEM for 15 min at 37°C. The mitochondrial ROS production was measured using flow cytometry (BD Biosciences) and quantified using FlowJo software (BD Biosciences). ATP content was evaluated using an ATP Determination kit (Invitrogen; Thermo Fisher Scientific, Inc.) according to the manufacturer's instructions using a multifunctional plate reader (BD Biosciences) at a wavelength of 650 nm. MDA release and SOD activity were determined using commercial kits (cat. nos. A003-1-2 and A001-3-2; Nanjing Jiancheng Bioengineering Institute) according to the manufacturer's instructions at a wavelength of 532 nm or 450 nm, respectively, using a multifunctional plate reader (BD Biosciences).

**Apoptosis analysis.** H9c2 cells ( $1 \times 10^6$  cells) were collected and resuspended in 500  $\mu$ l Annexin binding buffer to determine cell apoptosis using a Dead Cell Apoptosis kit with Annexin V Alexa Fluor<sup>™</sup> 488 and propidium iodide (PI) (Thermo Fisher Scientific, Inc.). The cells were incubated with FITC-conjugated Annexin V and PI each for 10 min at room temperature. A FACSCalibur instrument (BD Biosciences) was used to measure the levels of cell fluorescence. The data were analyzed using CellQuest<sup>™</sup> v5.1 software (BD Biosciences).

**RT-qPCR.** Total RNA was isolated from cells using TRIzol<sup>®</sup> reagent (Invitrogen; Thermo Fisher Scientific, Inc.). Subsequently, cDNA was synthesized using a Reverse Transcription kit (Takara Biotechnology Co., Ltd.) according to the manufacturer's instructions. qPCR was performed using SYBR<sup>®</sup> Premix Ex Taq (Takara Biotechnology Co., Ltd.) and an ABI 7500 system (Applied Biosystems; Thermo Fisher Scientific, Inc.). The following thermocycling conditions for PCR was used: 95°C for 5 min and then 40 cycles of 94°C for 15 sec, 55°C for 20 sec, 72°C for 20 sec, followed by 72°C for 7 min. The primers sequences used in the present study were as follows: NF- $\kappa$ B, forward, 5'-CTGAGTCCCGCCCTTCTAA-3' and reverse, 5'-CTCCACCAGCTCTTTGATGGT-3';

GAPDH, forward, 5'-ATGTGTCCGTCGTGGATCTGA-3' and reverse, 5'-GATGCCTGCTTACCACCTT-3'. The 2<sup>- $\Delta\Delta$ Ct</sup> method was carried out to compare relative expressions (21). GAPDH was considered as an internal reference gene.

**Western blotting.** Total proteins in cardiac tissues and H9c2 cells were isolated using RIPA reagent buffer (Beyotime Institute of Biotechnology) at 4°C and a BCA protein assay kit (Beyotime Institute of Biotechnology) was used to determine protein concentration. Equal amounts of protein (40  $\mu$ g per lane) were separated using SDS-PAGE (8-10% gel) and transferred to polyvinylidene difluoride (PVDF) membranes. Subsequently, 5% non-fat milk was used to block the membrane for 1 h at room temperature. The membrane was incubated with primary antibodies against PPAR $\alpha$  (cat. no. ab3484; 1:1,000; Abcam), cleaved-caspase-3 (cat. no. 9664; 1:1,000), caspase-3 (cat. no. 14220; 1:1,000), cleaved-caspase-9 (cat. no. 9057; 1:1,000), caspase-9 (cat. no. 9508; 1:1,000), cytochrome *c* (Cyt-*c*; cat. no. 11940T; 1:1,000), NF- $\kappa$ B (cat. no. 8242; 1:1,000) and GAPDH (cat. no. 5174; 1:1,000) (all from Cell Signaling Technology, Inc.) overnight at 4°C. The membranes were incubated with goat-anti-rabbit or goat-anti-mouse HRP-conjugated IgG (cat. nos. 7074 and 7076, respectively; 1:10,000; Cell Signaling Technology, Inc.) for 2 h at room temperature. The protein bands were visualized using an enhanced chemiluminescence detection system (Applygen Technologies, Inc.) and subsequently quantified using ImageJ software (version 1.52r; National Institutes of Health). GAPDH was used for normalization. Data are presented as relative levels compared with those in the control rats.

**Statistical analysis.** Data are presented as the mean  $\pm$  SD and were analyzed using GraphPad Prism 6.0 (GraphPad Software, Inc.). The statistical differences were calculated using one-way ANOVA followed by Tukey's post hoc test.  $P < 0.05$  was considered to indicate a statistically significant difference.

## Results

**Pemafibrate alleviates diabetic cardiac IRI.** STZ injections were used to induce the T1DM model in rats. Subsequently, the hearts were subjected to ischemia-reperfusion surgery to mimic cardiac IRI. TTC staining was performed to evaluate the extent of the infarction induced by diabetic IRI. Fig. 1A and B demonstrate that the infarct volume was significantly alleviated in rats treated with pemafibrate compared with that in rats in the D-IRI group. Immunohistochemical staining revealed that pemafibrate increased the protein expression levels of PPAR $\alpha$  compared with those in the D-IRI group (Fig. 1C). According to the TEM results, the D-IRI group displayed marked destruction of the intracellular structures including the myofibrils and mitochondria; the mitochondria were rounded, with a large space between cristae, and a number of mitochondria presented with membrane ruptures (Fig. 1D). The pemafibrate-treated group presented with intact mitochondria, which were irregularly arranged between the myofibrils, with normal striation of the cardiac muscle (Fig. 1D). These results suggest that pemafibrate increases PPAR $\alpha$  expression and may alleviate diabetic IRI.

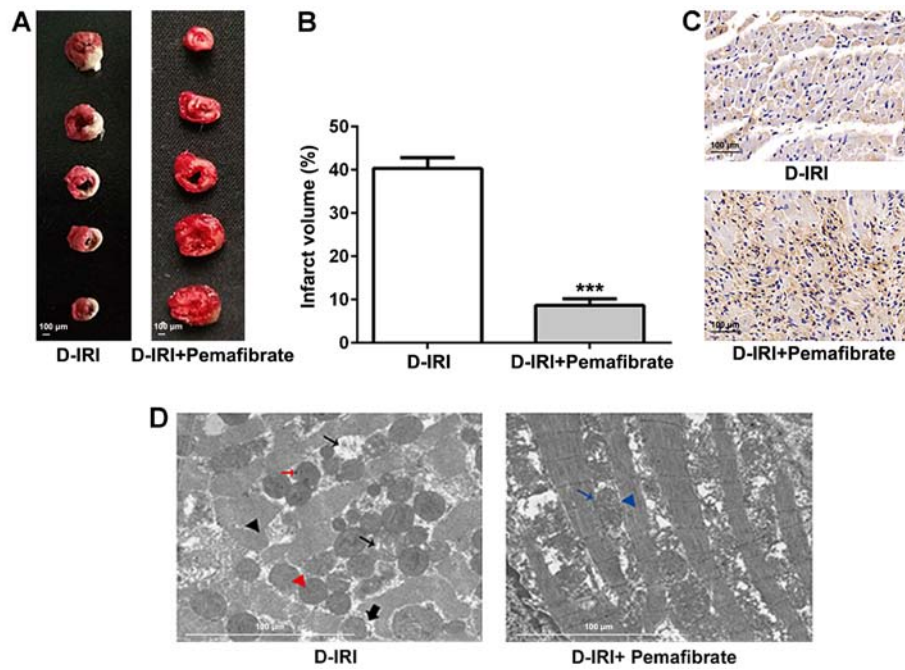


Figure 1. Effects of pemaifibrate on the extent of myocardial infarction and myocardial damage. (A and B) TTC staining of D-IRI induced infarction. (C) Immunohistochemistry for PPAR $\alpha$  expression in cardiac tissues. Magnification, x200. (D) The ultrastructure of myocardial tissue from the D-IRI and D-IRI + pemaifibrate groups revealed disrupted myofibrils (black arrowhead), rounded mitochondria with increased distance between cristae (small black arrow), electron-dense particles (red arrow), rupturing of the inner membranes resulting in protrusions from the mitochondria (thick black arrow), rupturing of the inner and outer membranes (red arrow head), normal mitochondria (blue arrow) and normal myofibrils (blue arrowhead). Scale bar, 100  $\mu$ m. \*\*\*P<0.001 vs. D-IRI. D-IRI, diabetic-myocardial ischemia reperfusion injury; PPAR $\alpha$ , peroxisome proliferator-activated receptor  $\alpha$ ; TTC, 2,3,5-triphenyltetrazolium chloride.

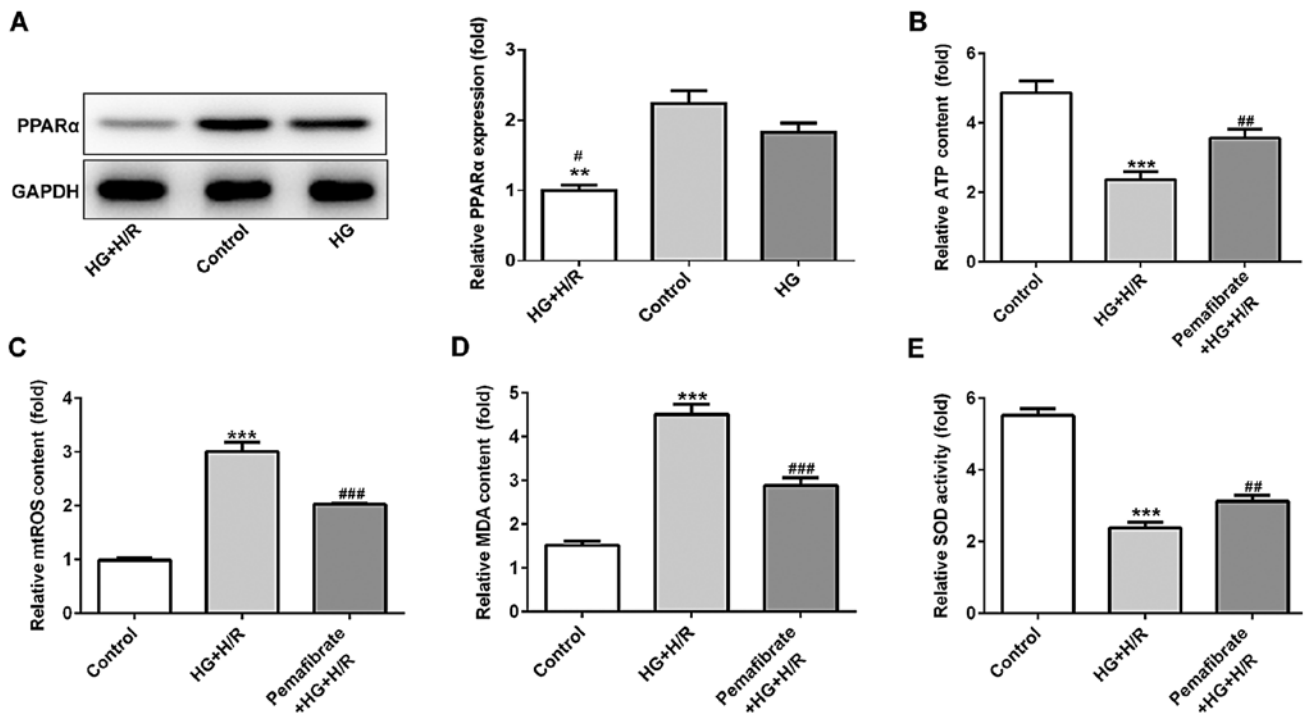


Figure 2. Pemaifibrate reduces mitochondrial dysfunction in H9c2 cells following H/R. (A) Protein expression levels of PPAR $\alpha$  under HG or HG + H/R conditions were detected by western blotting. \*\*P<0.01 vs. control; #P<0.05 vs. HG. (B-E) Relative levels of (B) ATP, (C) mtROS, (D) MDA and (E) SOD were determined using commercial assay kits. \*\*\*P<0.001 vs. control; \*\*P<0.01, \*\*\*P<0.001 vs. HG + H/R. HG, high glucose; H/R, hypoxia/reperfusion; MDA, malondialdehyde; mtROS, mitochondrial reactive oxygen species; PPAR $\alpha$ , peroxisome proliferator-activated receptor  $\alpha$ ; SOD, superoxide dismutase.

*Pemaifibrate inhibits mitochondrial dysfunction by increasing PPAR $\alpha$  expression.* H9c2 cells were treated with HG and

subsequently with H/R treatment to mimic diabetic IRI *in vitro*. The expression levels of PPAR $\alpha$  were evaluated using western

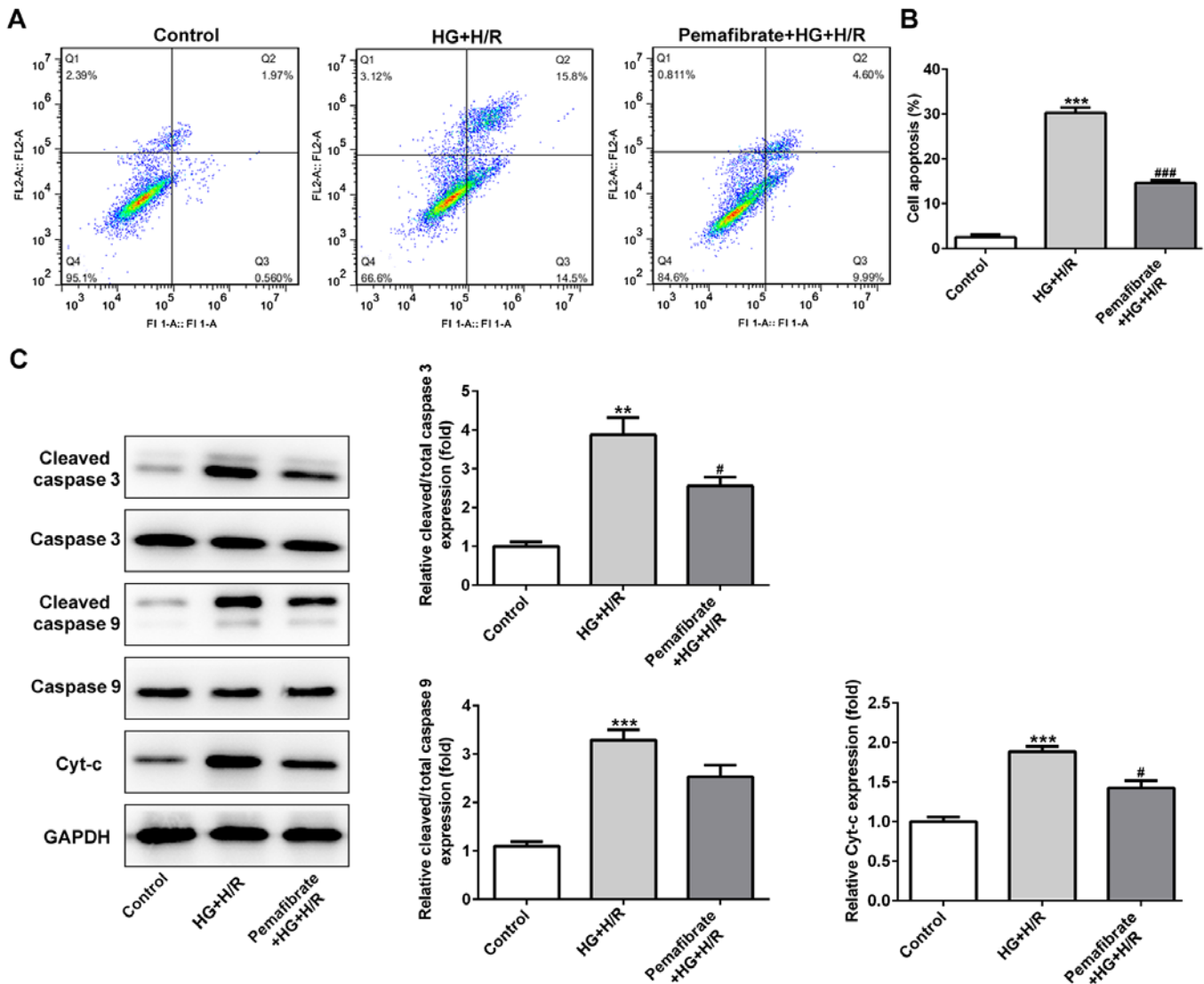


Figure 3. Pemaifibrate inhibits mitochondria-dependent apoptosis in H9c2 cells exposed to high glucose conditions following H/R. (A) Flow cytometry was performed to detect and (B) quantify apoptotic cells using FITC-Annexin V and propidium iodide staining. (C) The expression levels of apoptosis-related proteins were evaluated using western blotting. \*\* $P < 0.01$ , \*\*\* $P < 0.001$  vs. control; # $P < 0.05$ , ### $P < 0.001$  vs. HG + H/R. H/R, hypoxia/reperfusion; HG, high glucose; Cyt-c, cytochrome *c*.

blotting in the control, HG and HG + H/R groups. The results demonstrated that PPAR $\alpha$  protein expression levels were downregulated under HG conditions compared with those in the control group, although there was no significant difference found, while H/R treatment significantly exacerbated this reduction ( $P < 0.05$ ; Fig. 2A). As the mitochondria are the major energy producers (through the production of ATP) that use oxygen in cells, the ATP activity in treated and untreated H9c2 cells was investigated. The results demonstrated that compared with those in the control group, the relative ATP levels were reduced under HG + H/R treatment, whereas pemaifibrate significantly increased the ATP levels in HG and H/R conditions ( $P < 0.01$ ; Fig. 2B). The relative mtROS levels were enhanced by HG + H/R treatment compared with those in the control group ( $P < 0.001$ ; Fig. 2C), while pemaifibrate intervention notably reversed the level of mtROS relative to the HG + H/R group ( $P < 0.001$ ; Fig. 2C). To determine the potential protective effects of pemaifibrate on oxidative stress, the levels of MDA and SOD activity were examined; compared

with those in cells under HG + H/R conditions, treatment with pemaifibrate significantly decreased the MDA levels and increased the SOD activity ( $P < 0.001$  and  $P < 0.01$ , respectively; Fig. 2D and E).

#### *Pemaifibrate suppresses mitochondria-induced apoptosis.*

To assess whether pemaifibrate affected cell death under HG and H/R conditions, apoptotic rates were determined in the HG + H/R-treated H9c2 cells using flow cytometry. Compared with that in the control group, the apoptotic rate was significantly enhanced in the HG + H/R group, whereas treatment with pemaifibrate decreased the number of apoptotic cells ( $P < 0.001$ ; Fig. 3A and B). Hyperglycemia and H/R treatment also increased the protein levels of cleaved-caspase-3 and Cyt-c in H9c2 cells compared with those in the control cells ( $P < 0.01$ ; Fig. 3C), which was significantly reversed by pemaifibrate treatment ( $P < 0.05$ ; Fig. 3C). The levels of cleaved-caspase-9 in the HG + H/R group were increased compared with those in the control group, and they also appeared to be suppressed

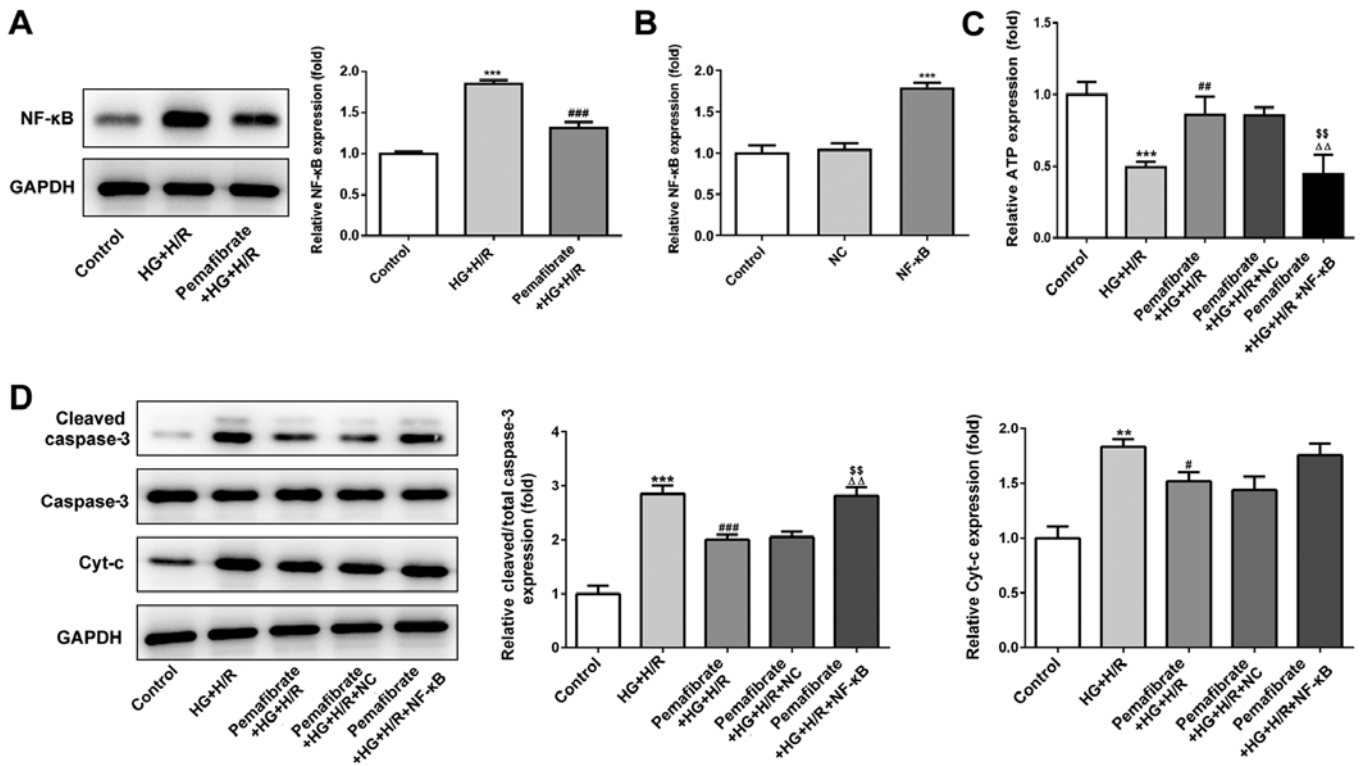


Figure 4. The biological effects of pemaifibrate treatment may be mediated by NF- $\kappa$ B signaling. (A) Protein expression levels of NF- $\kappa$ B were detected by western blotting. \*\*\* $P$ <0.001 vs. control; ### $P$ <0.001 vs. HG + H/R. (B) NF- $\kappa$ B expression was evaluated by reverse transcription-quantitative PCR following transfection. \*\*\* $P$ <0.001 vs. NC. (C) Relative levels of ATP were detected using commercial kits. (D) The expression levels of apoptosis-related proteins were assessed by western blotting. \*\* $P$ <0.01, \*\*\* $P$ <0.001 vs. control; # $P$ <0.05, ### $P$ <0.001 vs. HG + H/R;  $\Delta\Delta$  $P$ <0.01 vs. pemaifibrate-treated HG + H/R;  $^{SS}$  $P$ <0.01 vs. pemaifibrate-treated HG + I/R negative control. HG, high glucose; H/R, hypoxia/reperfusion; Cyt-c, cytochrome c; NF- $\kappa$ B, nuclear factor- $\kappa$ B; NC, negative control.

by pemaifibrate, although the difference was not significant (Fig. 3C).

*Pemaifibrate prevents mitochondrial dysfunction via the NF- $\kappa$ B signaling pathway.* Under HG + H/R conditions, NF- $\kappa$ B protein expression levels were significantly enhanced in H9c2 cells compared with those in the control group ( $P$ <0.001; Fig. 4A). Pemaifibrate significantly suppressed the protein expression levels of NF- $\kappa$ B compared with those in the HG + H/R group ( $P$ <0.001; Fig. 4A). To evaluate whether pemaifibrate may regulate mitochondrial dysfunction and apoptosis through the NF- $\kappa$ B signaling pathway, NF- $\kappa$ B was overexpressed in H9c2 cells ( $P$ <0.001; Fig. 4B). The results demonstrated that overexpression of NF- $\kappa$ B reversed the pemaifibrate-induced increase in ATP levels in the HG + H/R treatment group ( $P$ <0.01 vs. pemaifibrate + HG + H/R and pemaifibrate + HG + H/R + NC; Fig. 4C). Pemaifibrate decreased the expression levels of cleaved-caspase-3 compared with those in the HG + H/R group; however, overexpression of NF- $\kappa$ B reversed this effect ( $P$ <0.01 vs. pemaifibrate + HG + H/R and pemaifibrate + HG + H/R + NC; Fig. 4D), indicating that pemaifibrate inhibited the HG + H/R-induced apoptosis by regulating the NF- $\kappa$ B signaling pathway. However, overexpression of NF- $\kappa$ B expression failed to significantly reverse the pemaifibrate-induced reduction in Cyt-c expression levels (Fig. 4D). These results suggest that pemaifibrate may prevent mitochondrial dysfunction by interacting with the NF- $\kappa$ B signaling pathway.

## Discussion

In the present study, pemaifibrate was demonstrated to protect H9c2 cells against IRI and exposure to HG *in vitro*, as well as to limit the extent of the myocardial infarct *in vivo* in T1DM model rats. TEM and functional analysis (including ROS, ATP, SOD and MDA analyses) indicated mitochondrial dysfunction following diabetic IRI *in vivo*. Additionally, immunohistochemistry analysis and western blotting results revealed that pemaifibrate exerted a protective effect against diabetic IRI through the activation of PPAR $\alpha$  *in vivo*. Therefore, the protective effects of pemaifibrate were likely due to PPAR $\alpha$  activation, which exerted antioxidative and antiapoptotic effects, thus, preventing further cardiac injury.

The expression levels of PPAR $\alpha$  have been reported to be decreased under high glucose conditions in an animal model of diabetes (22). Additionally, PPAR $\alpha$  is downregulated in the hearts of offspring from Ins2<sup>Akita</sup> mothers with elevated blood glucose concentration (23). In the present study, pemaifibrate was notably reduced the extent of cardiac infarction and enhanced the expression of PPAR $\alpha$  in the T1DM IR rat model, which was in agreement with a previous study that demonstrated that PPAR $\alpha$  activation reduced cardiac IRI (24). To determine how pemaifibrate may affect the myocardial IRI under diabetic conditions, the ultrastructure of the myocardium was evaluated in the present study and marked destruction of the intracellular structures were observed in the D-IRI group. Similar alterations about

myocardial injury and mitochondrial dysfunction in the diabetic IRI have been observed in other reports (25,26). *In vivo* analysis in the present study demonstrated that pemafibrate partially restored the mitochondrial structure in the myocardium. Furthermore, pemafibrate enhanced the ATP and SOD activity levels, and decreased ROS and MDA levels in the HG + H/R treated H9c2 cells.

Both diabetes and IRI induce oxidative stress and apoptosis in cardiomyocytes (27,28). Hyperglycemic conditions and IR damage the mitochondrial function to induce oxidative stress and apoptosis (29,30). In the present study, pemafibrate reduced apoptosis induced by high glucose and IR treatment. Cyt-c is an electron carrier in the mitochondrial electron transport chain (31). Under cellular stress such as high glucose or IR, Cyt-c release from mitochondria is a key step that leads to apoptosis, resulting in the formation of the apoptosome and caspase activation (32). Pemafibrate markedly reduced Cyt-c protein expression levels and the extent of apoptosis in the cells under HG + H/R conditions in the present study. Furthermore, the generation of ROS induces apoptosis through mitochondria-dependent pathways (33). Therefore, pemafibrate may reduce mitochondria-dependent apoptosis in H9c2 cells under HG + H/R.

Treatment with pemafibrate in the doses used in the present study did not significantly decrease the blood glucose levels in the D-IRI model rats (data not shown). Diabetes enhances the susceptibility of cardiomyocytes to IRI and disrupts the cellular signaling pathway responsible for conditioning-induced enhancement of resistance to cell death to remodel cardiac responses to IRI (34). The combination of pemafibrate and hypoglycemic agents may be an effective strategy for the treatment of D-IRI; however, this requires further study.

NF- $\kappa$ B is a transcription factor involved in diverse cellular activities, both in normal and pathological conditions, including inflammation and proliferation (35). A recent study has demonstrated that NF- $\kappa$ B activation is induced by diabetic metabolic disorders with myocardial IRI, whereas inhibition of NF- $\kappa$ B reverses D-IRI-induced apoptosis (36). The results of the present study suggested that pemafibrate inhibited the expression of NF- $\kappa$ B, whereas overexpression of NF- $\kappa$ B reversed the upregulation of ATP and the down-regulation of cleaved-caspase-3 levels after pemafibrate treatment. However, Cyt-c expression levels were not significantly enhanced by overexpression of NF- $\kappa$ B. Activation of PPAR $\alpha$  reverses the HG-induced increases in the expression levels of NF- $\kappa$ B and subsequently inhibits apoptosis in diabetic cardiomyopathy (37), indicating that NF- $\kappa$ B may mediate the effects of pemafibrate on mitochondrial dysfunction and apoptosis.

In conclusion, pemafibrate may be a potential therapeutic agent for the treatment of myocardial IRI under diabetic conditions and may alleviate the diabetic-myocardial IRI by preventing mitochondrial dysfunction and inhibiting cardiomyocyte apoptosis via inhibition of the NF- $\kappa$ B signaling pathway. The results of the present study further enriched the theoretical basis for clinical research into the use of pemafibrate for the treatment of myocardial IRI in patients with T1DM. However, the lack of a sham control group is a limitation of the present study and whether the present findings are applicable to type 2 diabetes remains to be further determined.

## Acknowledgements

Not applicable.

## Funding

No funding was received.

## Availability of data and materials

The datasets used and/or analyzed during the present study are available from the corresponding author on reasonable request.

## Authors' contributions

WL and JX designed the research, interpreted the data and performed the experiments. XG and XX collected the data and searched the literature. WL wrote the manuscript. YS analyzed and interpreted the data and revised the manuscript. All authors read and approval the final manuscript.

## Ethics approval and consent to participate

This experiment was approved by the Ethics Committee of Tianjin Teda Hospital, China (EC-20190722-1039).

## Patient consent for publication

Not applicable.

## Competing interests

The authors declare that they have no competing interests.

## References

1. Bhawal UK, Yoshida K, Kurita T, Suzuki M, Okada Y, Tewari N, Oka S, Kuboyama N and Hiratsuka K: Effects of 830 nm low-power laser irradiation on body weight gain and inflammatory cytokines in experimental diabetes in different animal models. *Laser Ther* 28: 257-265, 2019.
2. Odak M, Douedi S, Upadhyaya V, Fadhel M and Cosentino J: Focal neurological seizure due to hyperglycemic hyperosmolar non-ketotic syndrome in undiagnosed diabetes mellitus. *Cureus* 12: e9909, 2020.
3. Hegazy GA, Awan Z, Hashem E, Al-Ama N and Abunaji AB: Levels of soluble cell adhesion molecules in type 2 diabetes mellitus patients with macrovascular complications. *J Int Med Res* 48: 300060519893858, 2020.
4. Šimonienė D, Platūkiene A, Prakapienė E, Radzevičienė L and Veličkienė D: Insulin resistance in type 1 diabetes mellitus and its association with patient's micro- and macrovascular complications, sex hormones, and other clinical data. *Diabetes Ther* 11: 161-174, 2020.
5. Guan Y, Zhou L, Zhang Y, Tian H, Li A and Han X: Effects of PP2A/Nrf2 on experimental diabetes mellitus-related cardiomyopathy by regulation of autophagy and apoptosis through ROS dependent pathway. *Cell Signal* 62: 109339, 2019.
6. Low Wang CC, Hess CN, Hiatt WR and Goldfine AB: Clinical update: Cardiovascular disease in diabetes mellitus: Atherosclerotic cardiovascular disease and heart failure in type 2 diabetes mellitus-mechanisms, management, and clinical considerations. *Circulation* 133: 2459-2502, 2016.
7. Dehaini H, Awada H, El-Yazbi A, Zouein FA, Issa K, Eid AA, Ibrahim M, Badran A, Baydoun E, Pintus G and Eid AH: MicroRNAs as potential pharmaco-targets in ischemia-reperfusion injury compounded by diabetes. *Cells* 8: 152, 2019.

8. Russo I, Penna C, Musso T, Popara J, Alloatti G, Cavalot F and Pagliaro P: Platelets, diabetes and myocardial ischemia/reperfusion injury. *Cardiovasc Diabetol* 16: 71, 2017.
9. Lam VH, Zhang L, Huqi A, Fukushima A, Tanner BA, Onay-Besikci A, Keung W, Kantor PF, Jaswal JS, Rebeyka IM and Lopaschuk GD: Activating PPAR $\alpha$  prevents post-ischemic contractile dysfunction in hypertrophied neonatal hearts. *Circ Res* 117: 41-51, 2015.
10. Yue TL, Bao W, Jucker BM, Gu JL, Romanic AM, Brown PJ, Cui J, Thudium DT, Boyce R, Burns-Kurtis CL, *et al*: Activation of peroxisome proliferator-activated receptor- $\alpha$  protects the heart from ischemia/reperfusion injury. *Circulation* 108: 2393-2399, 2003.
11. Song JW, Kim HJ, Lee H, Kim JW and Kwak YL: Protective effect of peroxisome proliferator-activated receptor  $\alpha$  activation against cardiac ischemia-reperfusion injury is related to upregulation of uncoupling protein-3. *Oxid Med Cell Longev* 2016: 3539649, 2016.
12. Panagia M, Gibbons GF, Radda GK and Clarke K: PPAR- $\alpha$  activation required for decreased glucose uptake and increased susceptibility to injury during ischemia. *Am J Physiol Heart Circ Physiol* 288: H2677-H2683, 2005.
13. Fu ZH, Mui D, Zhu H and Zhang Y: Exenatide inhibits NF- $\kappa$ B and attenuates ER stress in diabetic cardiomyocyte models. *Aging (Albany NY)* 12: 8640-8651, 2020.
14. Li L, Luo W, Qian YY, Zhu W, Qian J, Li J, Jin Y, Xu X and Liang G: Luteolin protects against diabetic cardiomyopathy by inhibiting NF- $\kappa$ B-mediated inflammation and activating the Nrf2-mediated antioxidant responses. *Phytomedicine* 59: 152774, 2019.
15. Jiang W, Cai X, Xu T, Liu K, Yang D, Fan L, Li G and Yu X: Tripartite motif-containing 46 promotes viability and inhibits apoptosis of osteosarcoma cells by activating NF-B signaling through ubiquitination of PPAR. *Oncol Res* 28: 409-421, 2020.
16. Araki E, Yamashita S, Arai H, Yokote K, Satoh J, Inoguchi T, Nakamura J, Maegawa H, Yoshioka N, Tanizawa Y, *et al*: Effects of pemafibrate, a novel selective PPAR $\alpha$  modulator, on lipid and glucose metabolism in patients with type 2 diabetes and hypertriglyceridemia: A randomized, double-blind, placebo-controlled, phase 3 trial. *Diabetes Care* 41: 538-546, 2018.
17. Tomita Y, Lee D, Miwa Y, Jiang X, Ohta M, Tsubota K and Kurihara T: Pemafibrate protects against retinal dysfunction in a murine model of diabetic retinopathy. *Int J Mol Sci* 21: 6243, 2020.
18. Pradhan AD, Paynter NP, Everett BM, Glynn RJ, Amarenco P, Elam M, Ginsberg H, Hiatt WR, Ishibashi S, Koenig W, *et al*: Rationale and design of the pemafibrate to reduce cardiovascular outcomes by reducing triglycerides in patients with diabetes (PROMINENT) study. *Am Heart J* 206: 80-93, 2018.
19. Zhang D, He Y, Ye X, Cai Y, Xu J, Zhang L, Li M, Liu H, Wang S and Xia Z: Activation of autophagy inhibits nucleotide-binding oligomerization domain-like receptor  $\alpha$  protein 3 inflammasome activation and attenuates myocardial ischemia-reperfusion injury in diabetic rats. *J Diabetes Investig* 11: 1126-1136, 2020.
20. Srisowanna N, Chojjookhuu N, Yano K, Batmunkh B, Ikenoue M, Nhat Huynh Mai N, Yamaguchi Y and Hishikawa Y: The effect of estrogen on hepatic fat accumulation during early phase of liver regeneration after partial hepatectomy in rats. *Acta Histochem Cytochem* 52: 67-75, 2019.
21. Livak KJ and Schmittgen TD: Analysis of relative gene expression data using real-time quantitative PCR and the 2(-Delta Delta C(T)) method. *Methods* 25: 402-408, 2001.
22. Hu Y, Chen Y, Ding L, He X, Takahashi Y, Gao Y, Shen W, Cheng R, Chen Q, Qi X, *et al*: Pathogenic role of diabetes-induced PPAR $\alpha$ - down-regulation in microvascular dysfunction. *Proc Natl Acad Sci USA* 110: 15401-15406, 2013.
23. Lindegaard ML and Nielsen LB: Maternal diabetes causes coordinated down-regulation of genes involved with lipid metabolism in the murine fetal heart. *Metabolism* 57: 766-773, 2008.
24. Qi K, Li X, Geng Y, Cui H, Jin C, Wang P, Li Y and Yang Y: Tongxinluo attenuates reperfusion injury in diabetic hearts by angiopoietin-like 4-mediated protection of endothelial barrier integrity via PPAR $\alpha$ - pathway. *PLoS One* 13: e0198403, 2018.
25. Muráriková M, Ferko M, Waczulíková I, Jašová M, Kancirová I, Murínová J and Ravingerová T: Changes in mitochondrial properties may contribute to enhanced resistance to ischemia-reperfusion injury in the diabetic rat heart. *Can J Physiol Pharmacol* 95: 969-976, 2017.
26. Yu L, Gong B, Duan W, Fan C, Zhang J, Li Z, Xue X, Xu Y, Meng D, Li B, *et al*: Melatonin ameliorates myocardial ischemia/reperfusion injury in type 1 diabetic rats by preserving mitochondrial function: Role of AMPK-PGC-1 $\alpha$ -SIRT3 signaling. *Sci Rep* 7: 41337, 2017.
27. Wilson AJ, Gill EK, Abudalo RA, Edgar KS, Watson CJ and Grieve DJ: Reactive oxygen species signalling in the diabetic heart: Emerging prospect for therapeutic targeting. *Heart* 104: 293-299, 2018.
28. Zhang M, Zhu J, Qin X, Zhou M, Zhang X, Gao Y, Zhang T, Xiao D, Cui W and Cai X: Cardioprotection of tetrahedral DNA nanostructures in myocardial ischemia-reperfusion injury. *ACS Appl Mater Interfaces* 11: 30631-30639, 2019.
29. Hou J, Zheng D, Xiao W, Li D, Ma J and Hu Y: Mangiferin enhanced autophagy via inhibiting mTORC1 pathway to prevent high glucose-induced cardiomyocyte injury. *Front Pharmacol* 9: 383, 2018.
30. Zhou H, Toan S, Zhu P, Wang J, Ren J and Zhang Y: DNA-PKcs promotes cardiac ischemia reperfusion injury through mitigating BI-1-governed mitochondrial homeostasis. *Basic Res Cardiol* 115: 11, 2020.
31. Wang X, Tang D, Zou Y, Wu X, Chen Y, Li H, Chen S, Shi Y and Niu H: A mitochondrial-targeted peptide ameliorated podocyte apoptosis through a HOCl-alb-enhanced and mitochondria-dependent signalling pathway in diabetic rats and in vitro. *J Enzym Inhib Med Chem* 34: 394-404, 2019.
32. Kalpage HA, Wan J, Morse PT, Zurek MP, Turner AA, Khobeir A, Yazdi N, Hakim L, Liu J, Vaishnav A, *et al*: Cytochrome c phosphorylation: Control of mitochondrial electron transport chain flux and apoptosis. *Int J Biochem Cell Biol* 121: 105704, 2020.
33. Sinha K, Das J, Pal PB and Sil PC: Oxidative stress: The mitochondria-dependent and mitochondria-independent pathways of apoptosis. *Arch Toxicol* 87: 1157-1180, 2013.
34. Lejay A, Fang F, John R, Van JA, Barr M, Thaveau F, Chakfe N, Geny B and Scholey JW: Ischemia reperfusion injury, ischemic conditioning and diabetes mellitus. *J Mol Cell Cardiol* 91: 11-22, 2016.
35. Wen Y, Geng L, Zhou L, Pei X, Yang Z and Ding Z: Betulin alleviates on myocardial inflammation in diabetes mice via regulating Sirt1/NLRP3/NF- $\kappa$ B pathway. *Int Immunopharmacol* 85: 106653, 2020.
36. Liu Y, Wang T, Zhang M, Chen P and Yu Y: Down-regulation of myocardial infarction associated transcript 1 improves myocardial ischemia-reperfusion injury in aged diabetic rats by inhibition of activation of NF- $\kappa$ B signaling pathway. *Chem Biol Interact* 300: 111-122, 2019.
37. Nan WQ, Shan TQ, Qian X, Ping W, Bing GA and Ying LL: PPAR $\alpha$  agonist prevented the apoptosis induced by glucose and fatty acid in neonatal cardiomyocytes. *J Endocrinol Invest* 34: 271-275, 2011.



This work is licensed under a Creative Commons Attribution-NonCommercial-NoDerivatives 4.0 International (CC BY-NC-ND 4.0) License.